ELSEVIER

Journal of Nuclear Materials 283–287 (2000) 731–735

journal of nuclear materials

www.elsevier.nl/locate/jnucmat

The mechanical properties and microstructure of the OPTIMAX series of low activation ferritic–martensitic steels

N. Baluc *, R. Schäublin, C. Bailat, F. Paschoud, M. Victoria

Centre of Research in Plasma Physics, Swiss Federal Institute of Technology – Lausanne, Fusion Technology Materials Division, OVGA/6, 5232 Villigen-PSI, Switzerland

Abstract

Polycrystalline specimens of the ferritic–martensitic OPTIMAX A steel have been irradiated on the one hand with neutrons at 523 K to a dose of 2.5 dpa and with 590 MeV protons at ambient temperature and 523 K to doses of about 0.3 and 1 dpa on the other. Charpy tests reveal a shift of the ductile-to-brittle transition temperature from about 190 to 268 K in the neutron-irradiated steel. Proton irradiations at ambient temperature lead to hardening and reduction of tensile ductility of the material. Both phenomena are strongly and positively dependent on dose. After irradiation at 523 K, they appear negligible (at least for the dose of 0.75 dpa). Transmission electron microscopy observations reveal that neutron irradiation leads to the formation of only a few visible black dots, together with a few faceted cavities, while proton irradiations also produce few visible defect clusters with sizes of about 1–2 nm, with no clear difference in size and density with dose and temperature. As a particular result, from proton irradiations performed at ambient temperature, the embedded carbides become amorphous, while at 523 K they remain crystalline.

1. Introduction

The low activation ferritic–martensitic steels known as OPTIMAX steels have been developed as candidate structural materials for the first wall of future fusion reactors [1]. They are based on the 9%Cr/W/V/Ta composition and a series of casts with different contents of W, Mn, Si and N have been produced from high purity components under clean processing conditions. The main difference between the different casts is that the steel designated as OPTIMAX A contains 0.56 wt% Mn and 0.0007 wt% N, while the conditions are reversed in alloy B, which contains 0.037 wt% Mn and 0.003 wt% N [1]. In OPTIMAX C and D, the W content was raised to 2 wt%, with a higher N content in the D alloy. A fine carbide structure has been obtained in all cases by normalizing the steels at 1370 K before austenization for 30 min at 1230–1250 K (depending on the steel composition) for obtaining a final pre-austenite grain size of 16–20 μm. After tempering at 1020 K (which was used as tempering temperature for all steel compositions) for 2 h, the carbide volume fraction in both OPTIMAX A and B steels is about 4%. The main difference between the two steels is due to the presence of a higher density of small carbides (<40 nm) in the higher nitrogen containing steel B. The resulting yield strengths range from 470 (OPTIMAX A) to 560 MPa (OPTIMAX C) at ambient temperature, to values as high as 450 MPa at 720 K [2]. The steel with the lowest ductile-to-brittle transition temperature (DBTT ≅ 190 K), OPTIMAX A, was chosen for the present investigation.

The present research is aimed at providing information about radiation effects on the mechanical behavior and microstructure of polycrystalline specimens of OPTIMAX A steel by combining Charpy experiments with conventional mechanical testing and transmission electron microscopy (TEM) observations. Results are tentatively compared with those previously obtained for polycrystalline specimens of ferritic–martensitic F82H steel, another low activation material (of slightly lower Cr and higher W content than OPTIMAX A) of promising interest, which was irradiated and deformed under similar conditions [3–6].

* Corresponding author. Tel.: +41-56 310 2975; fax: +41-56 310 4529.

E-mail address: nadine.baluc@psi.ch (N. Baluc).

0022-3115/00/$ - see front matter
PII: S0022-3115(00)00282-8

2. Experimental procedure

Series of Charpy and tensile flat specimens have been prepared from an austenized polycrystalline ingot of OPTIMAX A. All the Charpy specimens and a set of tensile specimens have been neutron-irradiated at 570 K in the research reactor at Petten to a dose of 2.5 dpa. All other tensile specimens were irradiated in the PIREX (*p*roton *ir*radiation *ex*periment) facility, at the Paul Scherrer Institute, with 590 MeV protons. These irradiations were performed at ambient temperature (300–320 K) and 523 K to doses of about 0.37 and 0.93 dpa, and 0.30 and 0.75 dpa, respectively. The damage rate was approximately 10^{-7} dpa s^{-1}.

Charpy tests were conducted at various temperatures ranging between 153 and 393 K. Tensile deformation experiments were conducted in vacuum, at the same temperature as the irradiation one, in a Schenck RMC100 deformation machine. The strain rate was about 6×10^{-5} s^{-1}.

Samples for TEM were sectioned from the irradiated Charpy specimens using a wire saw and punched from the irradiated tensile specimens. In order to reduce magnetism and radioactivity, TEM samples were prepared in a special way [7]. The defects associated with irradiation were imaged with a JEOL 2010 microscope operating at 200 kV by using the bright/dark field and weak beam techniques. In weak beam imaging, which was applied more specifically to the measurement of irradiation-induced defect cluster sizes and densities, specimens were tilted to $\boldsymbol{g}(4\boldsymbol{g})$ and $\boldsymbol{g}(6\boldsymbol{g})$ weak Bragg reflection conditions using diffraction vectors ($\boldsymbol{g}$) of the {1 1 0} type.

3. Results and discussion

3.1. Charpy tests

The effects of neutron irradiation at 523 K to a dose of 2.5 dpa on the temperature dependence of shelf energy and on the DBTT of OPTIMAX A are shown in Fig. 1. It can be seen that, while the DBTT value (measured at 1/2 USE) of unirradiated specimens is about 190 K with an upper shelf energy (USE) of about 9 J, it increases to about 268 K (leading to a ΔDBTT of 78 K) for irradiated specimens, while keeping nearly the same USE value. Note that dispersion of experimental results is much more important for the irradiated specimens than for the unirradiated ones. The ductile-to-brittle transition is also less sharp after irradiation. In case of the F82H steel, the DBTT was observed to shift from about 185 K for unirradiated specimens to 326 K for specimens irradiated with neutrons at 573 K to the same dose of 2.5 dpa [6]. Hence, the shift of DBTT appears much smaller for OPTIMAX A than for F82H,

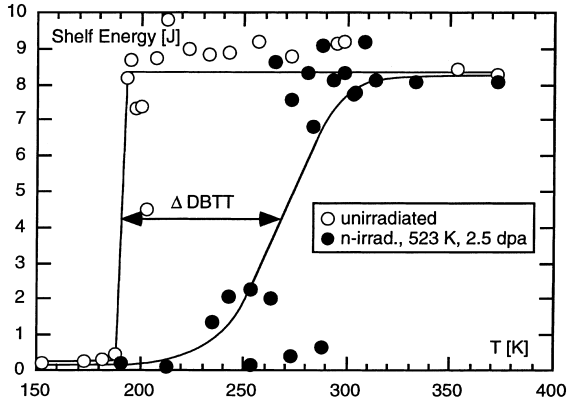

Fig. 1. Shelf energy as a function of temperature for unirradiated and neutron-irradiated Charpy specimens at 523 K to 2.5 dpa.

considering only doses $\leqslant 2.5$ dpa at 523 K. As pointed out in [1], nitrogen seems to strongly influence the microstructure, in the sense that a high N content seems to favor the formation of a high density of small carbides (nitrates or carbonitrates) and to rise strength levels. The different DBTT values found for OPTIMAX A and F82H can be explained on that basis, that is, a low N content (much lower in OPTIMAX A than in F82H) seems to promote a lower DBTT value.

3.2. Tensile mechanical testing

Fig. 2 shows tensile true stress–true strain curves of unirradiated specimens, which were deformed at ambient temperature and 523 K, and specimens irradiated with protons either at ambient temperature (to 0.37 and 0.93 dpa) or at 523 K (to 0.30 and 0.75 dpa) that were subsequently deformed at the same temperature as the irradiation one. Values of important parameters, like the

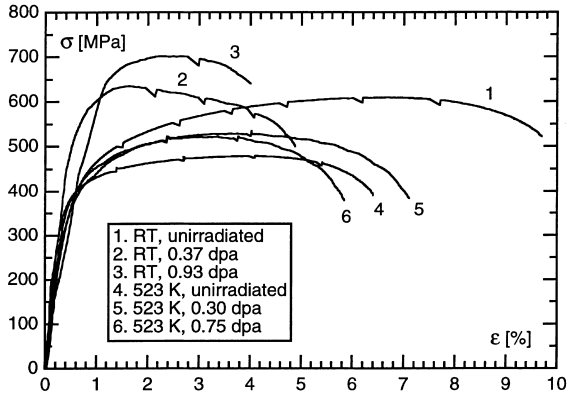

Fig. 2. Tensile true stress–true strain curves of unirradiated and proton-irradiated specimens ($T_{test} = T_{irrad.}$). The small jumps on the curves reveal the positions of load relaxation experiments.

Table 1
Results of tensile deformation experiments of unirradiated and proton-irradiated specimens[a]

Parameters	$\sigma_{0.2}$ (MPa)	σ_u (MPa)	σ_f (MPa)	ε_u (%)	ε_f (%)
Specimens					
Unirradiated, def. at 300 K	416	610	512	6.0	9.1
p-irrad., 300 K, 0.37 dpa	542	631	495	1.1	4.5
p-irrad., 300 K, 0.93 dpa	662	701	636	1.3	3.0
Unirradiated, def. at 523 K	385	480	385	3.6	6.1
p-irrad., 523 K, 0.30 dpa	392	529	376	3.1	6.7
p-irrad., 523 K, 0.75 dpa	412	521	377	2.8	5.4

[a] $\sigma_{0.2}$ is the true offset yield strength (measured at 0.2% plastic strain), σ_u the true ultimate tensile strength, σ_f the true fracture stress, ε_u the true uniform strain and ε_f is the true fracture strain.

true offset yield strength measured at 0.2% plastic strain ($\sigma_{0.2}$), the true ultimate tensile strength (σ_u) and the true fracture stress (σ_f), as well as the corresponding true strains (the uniform one, ε_u, and the fracture one, ε_f) have been taken from the different curves and reported in Table 1.

It can be seen from Fig. 2 and Table 1 that the tensile mechanical behavior of OPTIMAX A is strongly affected by proton irradiation at ambient temperature. In particular, a strong increase in $\sigma_{0.2}$ is observed, together with a decrease in ε_f. Both phenomena are strongly and positively dependent on dose. For instance, the irradiation hardening ($\Delta\sigma_{0.2}$, defined as the difference between $\sigma_{0.2}$ of irradiated and unirradiated specimens) increases from 126 MPa for a dose of 0.37 dpa to 246 MPa for 0.93 dpa, accompanied by a strong loss of tensile ductility ($\Delta\varepsilon_f$, defined as the difference in the total elongation of unirradiated and irradiated specimens) of 4.6% and 6.1%, respectively. On the other hand, the mechanical behavior of OPTIMAX A is comparably less affected by proton irradiations performed at 523 K. Indeed, a slight hardening is then observed, equal to 7 MPa for a dose of 0.30 dpa and 27 MPa for 0.75 dpa, together with a slight reduction of the total elongation only at the higher dose of 0.75 dpa. This is in strong contrast with the results of tensile tests performed on F82H specimens, where $\Delta\sigma_{0.2}$ values of 70 and 98 MPa were found after proton irradiation at 523 K to comparable doses of 0.26 and 0.45 dpa, respectively [2]. Values obtained for F82H specimens irradiated and subsequently deformed at ambient temperature vary from about 210 MPa for a dose of about 0.21 ± 0.5 dpa to 285 MPa for 1.74 dpa [3]. It indicates that the irradiation-induced hardening at ambient temperature of OPTIMAX A, which exhibits a $(\text{dose})^{1/3}$ dependence, follows the same trend as F82H, which was found to exhibit a $(\text{dose})^{1/4}$ dependence [4]. Experimentally, both behaviors are too close to be really distinguished.

3.3. Transmission electron microscopy investigation

Fig. 3 shows weak beam TEM images of the specimens investigated in this study using a $\boldsymbol{g}(6\boldsymbol{g})$ condition. Fig. 3(a), representing the as-received material OPTIMAX A, exhibits characteristic thickness fringes starting from the edge of the thin foil that is just visible at the right of the picture. A few dislocations are visible. Dislocation images have been recorded in all cases in order to give a diffraction contrast reference for the identification of 'black dot' contrasts. Fig. 3(b) represents OPTIMAX A irradiated with neutrons at 523 K to 2.5 dpa. Only a few black dot contrasts are observed in the background. This indicates that the defects induced by the neutron irradiation are of much lower density than that observed in the F82H ferritic–martensitic steel [7] for the same irradiation conditions. Interestingly it appears that there are a number of curved dislocations and loops that have a diameter of about 50 nm or more. In addition, faceted cavities have been observed with a mean size of 10 nm and a density of about 10^{20} m^{-3}.

Figs. 3(c) and (d) show OPTIMAX A proton-irradiated to 0.3 dpa at 300 and 523 K, respectively. Black dot contrasts are visible in the case of the low-temperature irradiation, while only a few dot contrasts can be envisaged as arising from defect clusters in the high temperature case. Figs. 3(e) and (f) show OPTIMAX A proton-irradiated to 0.7 dpa at 300 and 523 K, respectively. Again, black dot contrasts are visible in the case of the low-temperature irradiation, while only a few dot contrasts can be envisaged as arising from defect clusters in the high temperature case. It should be noted that it is difficult to draw a quantitative conclusion on the dose and temperature dependence of the size and density of these clusters because of the low numbers of their occurrence in the pictures. The black dots have sizes that, in all cases, lie between 1 and 2 nm.

Fig. 4 presents TEM images of two OPTIMAX specimens that were proton-irradiated at the same dose of 0.3 dpa and at two different irradiation temperatures of 523 and 300 K, respectively, for the top and bottom image rows. Fig. 4(a), presenting a bright field TEM image of the high-temperature irradiation, shows martensite lathes, the boundaries of which are decorated with carbides. Within the lathes, a high density of dislocations that can form, in some instances, a cell

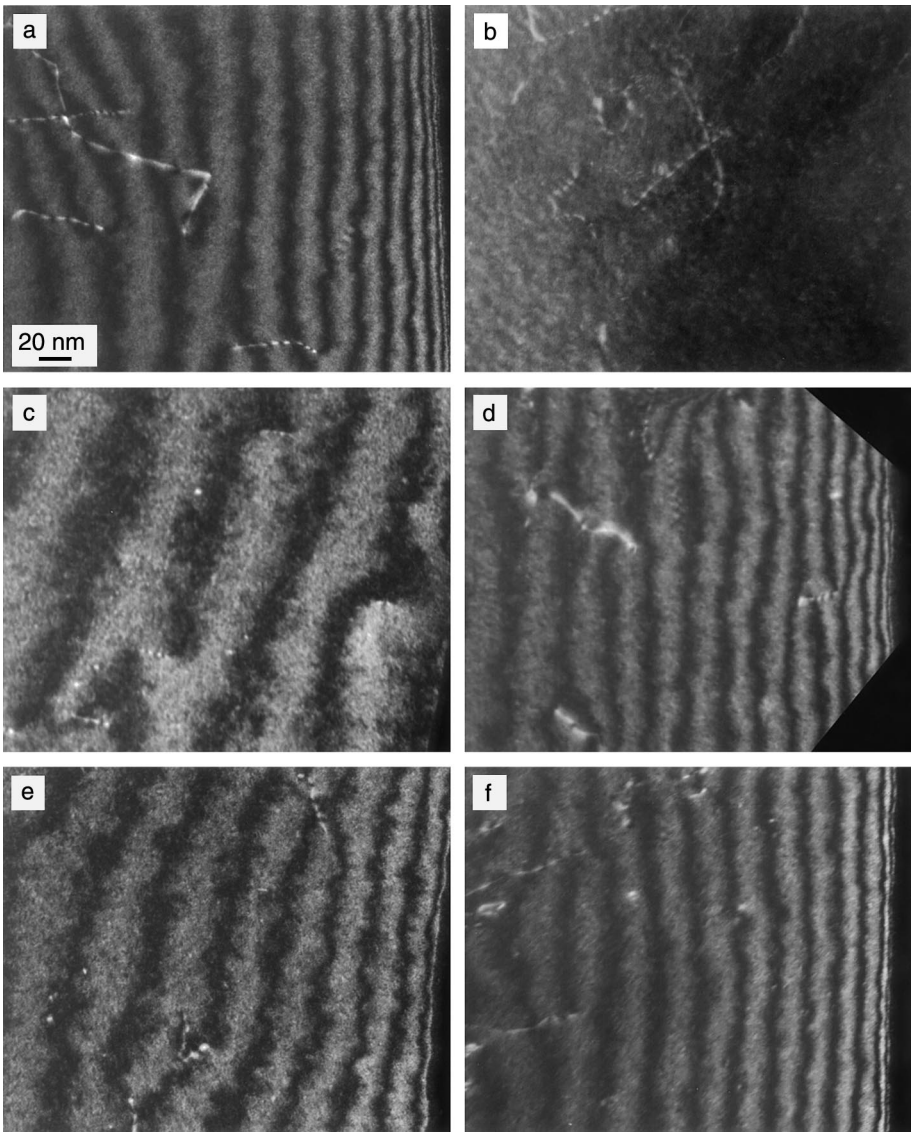

Fig. 3. Weak beam $\boldsymbol{g}(6\boldsymbol{g})$, $\boldsymbol{g} = \{1\,1\,0\}$. TEM images of the microstructure of (a) an unirradiated specimen, (b) a neutron-irradiated specimen at 523 K to 2.5 dpa, and proton-irradiated specimens (c) at 300 K to 0.3 dpa, (d) at 523 K to 0.3 dpa, (e) at 300 K to 0.7 dpa and (f) at 523 K to 0.7 dpa.

structure is visible. Fig. 4(b) presents the same area in dark field TEM with the objective aperture placed close to a $\{0\,1\,1\}$ diffraction spot. A few light areas appear that correspond to carbides. However, only a fraction of the carbides that can be identified in Fig. 4(a) present a light contrast. This fact, and the fact that the carbide light contrast is inhomogeneous, indicates that the carbides are crystalline.

Fig. 4(c), presenting a bright field TEM image of the low-temperature irradiation, shows a number of carbides embedded in the ferritic–martensitic material. Lath boundaries and the microstructure in general are less visible than in the previous case because the sample appears to be thinner here. The diffraction pattern, shown in Fig. 4(d), presents two concentric diffuse rings. The corresponding dark field, Fig. 4(d), shows that all carbides identified in Fig. 4(c) are in light contrast. This, and the fact that the carbide contrast is homogeneous, indicates that the carbides have been amorphized by the irradiation, as was observed earlier in another proton-irradiated ferritic steel [8]. In summary, it appears that, independent of the dose, the proton irradiations performed at ambient temperature amorphize the carbides, while at 523 K they remain crystalline.

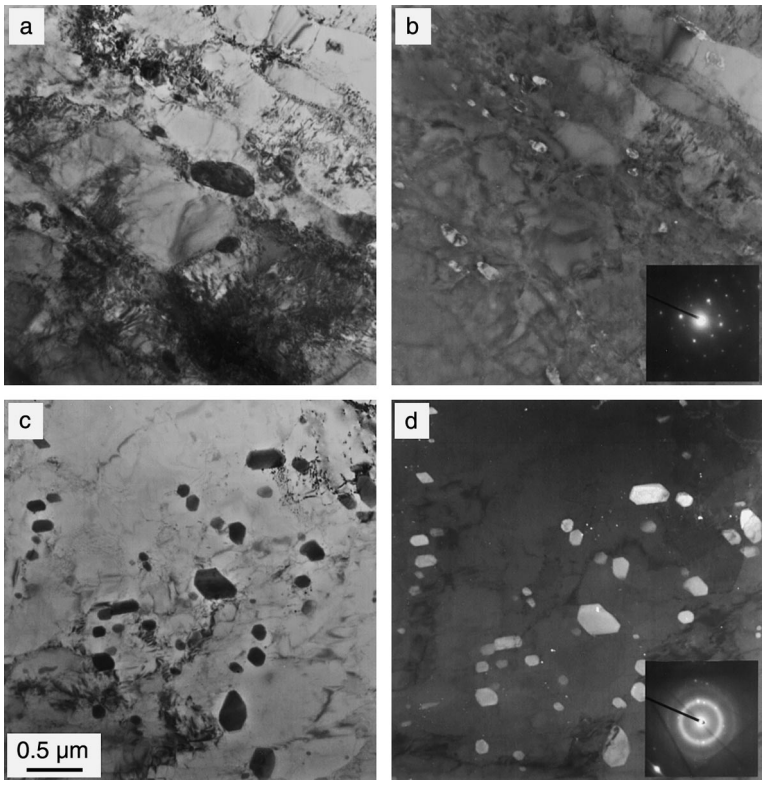

Fig. 4. (a) Bright field and (b) dark field TEM images of the microstructure of a proton-irradiated specimen at 523 K to 0.3 dpa, and (c) bright field and (d) dark field TEM images of the microstructure of a proton-irradiated specimen at 300 K to 0.3 dpa.

4. Conclusions

As previously found for F82H steel, high-energy proton irradiation (at ambient temperature and 523 K to doses ranging between 0.3 and 1 dpa) of OPTIMAX A steel induces hardening and reduces total elongation (related to the formation of small defect clusters and, perhaps, to carbide amorphization in the case of irradiations performed at ambient temperature). Neutron irradiation (at 523 K to a dose of 2.5 dpa) yields a shift of the DBTT value to higher temperatures and promotes the formation of cavities. However, these phenomena (DBTT shift and hardening by proton irradiation) are much less pronounced for OPTIMAX A than for F82H. Hardening appears even negligible for proton irradiations perfomed at 523 K, considering only doses $\leqslant 0.75$ dpa and $T_{\text{test}} = T_{\text{irrad.}} = 523$ K.

Acknowledgements

We gratefully acknowledge EURATOM and the Swiss National Science Foundation for providing financial support, and the Paul Scherrer Institute for the overall use of the facilities.

References

[1] M. Victoria, E. Batawi, Ch. Briguet, D. Gavillet, P. Marmy, J. Peters, F. Rézai-Aria, in: D.S. Gelles et al. (Eds.), Proceedings of the 17th ASTM Symposium on Effects of Radiation on Materials, ASTM, Philadelphia, 1995, p. 721.
[2] N. Baluc, C. Bailat, M. Victoria, to be published.
[3] P. Spätig, R. Schäublin, S. Gyger, M. Victoria, J. Nucl. Mater. 258–263 (1998) 1345.
[4] N. Baluc, C. Bailat, Y. Dai, M.I. Luppo, R. Schäublin, M. Victoria, in: D.G. Lucas et al. (Eds.), MRS Symposium Proceedings on Microstructural Processes in Irradiated Materials, MRS, Pittsburgh, PA, 1999, vol. 540, p. 539.
[5] R. Schäublin, P. Spätig, M. Victoria, J. Nucl. Mater. 258–263 (1998) 1178.
[6] E.V. van Osch, in: R.L. Klueh (Ed.), Proceedings of the IEA Workshop/Working Group Meeting on Ferritic/Martensitic Steels, Petten, Netherlands, 1998.
[7] R. Schäublin, M. Victoria, these Proceedings, p. 339.
[8] Y. Dai, G.S. Bauer, F. Carsughi, H. Ullmaier, S.A. Maloy, W.F. Sommer, J. Nucl. Mater. 265 (1999) 203.